Dynamic Structure Factor of Poly(*n*-hexyl isocyanate) in Dilute Solution

Naoki Yoshida, Takenao Yoshizaki, and Hiromi Yamakawa*

Department of Polymer Chemistry, Kyoto University, Kyoto 606-8501, Japan

Received December 10, 1999; Revised Manuscript Received February 14, 2000

ABSTRACT: The first cumulant $\Omega(k)$ of the dynamic structure factor as a function of the magnitude k of the scattering vector was determined from dynamic light scattering measurements for three poly(*n*-hexyl isocyanate) (PHIC) samples with weight-average molecular weights equal to 1.04×10^5, 3.63×10^5, and 7.71×10^5 in *n*-hexane at 25.0 °C. The mean-square radius of gyration $\langle S^2 \rangle$, the translational diffusion coefficient, and the intrinsic viscosity were also determined from static and dynamic light scattering and viscosity measurements, respectively, to characterize the samples. It is shown that the present data for PHIC as a typical semiflexible polymer along with the previous data for atactic polystyrene and the literature data for DNA are consistent with the theoretical prediction on the basis of the helical wormlike chain model for the dimensionless quantity $\eta_0\Omega(k)/k_BTk^3$ as a function of the reduced magnitude $\langle S^2 \rangle^{1/2}k$ of the scattering vector, where η_0 is the solvent viscosity, k_B the Boltzmann constant, and T the absolute temperature. In general, this dimensionless quantity appreciably depends on the kind of polymer even for flexible polymers.

Introduction

Recently, the first cumulant Ω of the dynamic structure factor has been evaluated theoretically for both flexible and semiflexible polymers in dilute solution[1] on the basis of the helical wormlike (HW) chain model.[2,3] The following two remarkable conclusions have then been deduced from the theory. First, for flexible polymers with very high molecular weights in Θ solvents, the so-called universal plot of $\eta_0\Omega(k)/k_BTk^3$ against $\langle S^2 \rangle^{1/2}k$ is not necessarily universal, where η_0 is the solvent viscosity, k_B the Boltzmann constant, T the absolute temperature, k the magnitude of the scattering vector, and $\langle S^2 \rangle$ the mean-square radius of gyration. Second, for semiflexible polymers, for which there is not essentially such universality, the plot appreciably depends on chain stiffness. The former prediction has very recently been confirmed experimentally by a comparison between the plots for atactic polystyrene (a-PS) and atactic poly(methyl methacrylate).[4] Thus, the purpose of the present paper is to make a comparison of theory with experiment with respect to Ω for semiflexible polymers.

We choose as a test semiflexible polymer poly(*n*-hexyl isocyanate) (PHIC), since its dilute solution properties such as $\langle S^2 \rangle$, the intrinsic viscosity $[\eta]$, and the sedimentation coefficient s have already been thoroughly investigated and the model parameters of this polymer as the Kratky−Porod (KP) wormlike chain[2,5] have been accurately determined.[6] The KP chain as a special case of the HW chain[2] may be described in terms of two basic model parameters: the static stiffness parameter λ^{-1} and the shift factor M_L as defined as the molecular weight per unit contour length. In addition to these two parameters, the hydrodynamic thickness of the chain is required if we consider its transport properties. The HW theory of Ω shows that its behavior is closely related to the translational diffusion coefficient D, especially in the range of small k. It is therefore desirable to perform our experiments using a solvent in which the hydrodynamic chain thickness has already been determined from D (or s), and also λ^{-1} and M_L have been determined from $\langle S^2 \rangle$. Thus, we choose as a solvent *n*-hexane and carry out measurements at 25.0 °C.[6]

In anticipation of the results, it is pertinent here to make some remarks on possible effects of the preaveraging approximation to the Oseen hydrodynamic interaction tensor[2] made in the HW theory. As previously mentioned,[1,4] in the case of flexible polymers, the effects are 2-fold, that is, one on the entire translational motion and the other on internal motions. The former, which was first pointed out by Zimm,[7] leads to an overestimate (about 13%) of the theoretical D, and hence Ω, in the range of small k,[2,8] while the latter leads to an underestimate of Ω in the range of large k.[9,10] On the other hand, in the case of semiflexible polymers, the former is immaterial,[2,8] so that the theory may be considered to only underestimate Ω in the range of large k.

Experimental Section

Materials. The original PHIC samples were prepared following the procedure of Aharoni.[11] The polymerization was carried out in a toluene/*N*,*N*-dimethylformamide (1:1) mixture at −78 °C with sodium cyanide as an initiator and methanol as a terminator. The three test samples PHIC10, PHIC36, and PHIC77 are fractions separated from the original samples by fractional precipitation using benzene as a solvent and methanol as a precipitant.

The solvent *n*-hexane used for all measurements was purified according to a standard procedure prior to use.

Static Light Scattering. Static light scattering (SLS) measurements were carried out to determine the weight-average molecular weight M_w and $\langle S^2 \rangle$ for all the samples in *n*-hexane at 25.0 °C. A Fica 50 light scattering photometer was used for all the measurements with vertically polarized incident light of wavelength $\lambda_0 = 436$ nm. For a calibration of the apparatus, the intensity of light scattered from pure benzene was measured at 25.0 °C at a scattering angle θ of 90°, where the Rayleigh ratio $R_{U_u}(90°)$ of pure benzene was taken as 46.5×10^{-6} cm^{-1}.[12] The depolarization ratio ρ_u of pure benzene at 25.0 °C was found to be 0.41 ± 0.01. Scattered intensities were measured at four different concentrations for PHIC10 and at five concentrations for PHIC36 and PHIC77 and at θ ranging from 30° to 105° for PHIC10, from 22.5° to 45° for PHIC36, and from 20° to 35° for PHIC77. All the data

10.1021/ma992075x CCC: $19.00 © 2000 American Chemical Society
Published on Web 04/10/2000

Table 1. Values of M_w and M_w/M_n for Poly(*n*-hexyl isocyanate)

sample	M_w	M_w/M_n
PHIC10	1.04×10^5	1.03
PHIC36	3.63×10^5	1.07
PHIC77	7.71×10^5	1.09

obtained were analyzed by the Berry square-root plot[13] with the use of the literature value[14] 0.134 cm^3/g of the refractive index increment for PHIC in *n*-hexane at 25.0 °C along with the value 1.380 of the refractive index n_0 of *n*-hexane at 25.0 °C, both at $\lambda_0 = 436$ nm. We note that the optical anisotropy for the three samples is negligibly small if any.[14]

The most concentrated solution of each sample was prepared gravimetrically and made homogeneous by continuous stirring at ca. 50 °C for 1 or 2 days. It was optically purified by filtration through a Teflon membrane of pore size 0.45 μm for PHIC10, 1.0 μm for PHIC36, and 2.0 μm for PHIC77. The solutions of lower concentrations were obtained by successive dilution, adding the solvent optically purified by filtration through a Teflon membrane of pore size 0.1 μm. The weight concentrations of the test solutions were converted to the polymer mass concentrations c by the use of the densities of the solutions.

The values of M_w thus determined and the ratio of M_w to the number-average molecular weight M_n determined by analytical GPC are given in Table 1.

Dynamic Light Scattering. Dynamic light scattering (DLS) measurements were carried out to determine D and $\Omega(k)$ for all the samples in *n*-hexane at 25.0 °C by the use of a Brookhaven Instruments model BI-200SM light scattering goniometer with vertically polarized incident light of $\lambda_0 = 488$ nm from a Spectra-Physics model 2020 argon ion laser equipped with a model 583 temperature-stabilized etalon for single-frequency-mode operation. The photomultiplier tube used was EMI 9863B/350, the output from which was processed by a Brookhaven Instruments model BI2030AT autocorrelator with 264 channels. (An electric shutter was attached to the original detector alignment to monitor the dark count automatically.) The method of data analysis for D is the same as that described in previous papers.[15,16] As for Ω, the CONTIN method[17] was employed as before.[4]

For the determination of D for each sample, the normalized autocorrelation function $g^{(2)}(t)$ of the scattered light intensity was measured at four concentrations and at θ ranging from 14° to 22° for PHIC10 and PHIC36 and from 14° to 18° for PHIC77. For the determination of $\Omega(k)$, it was measured at θ = 20°, 25°, 30°, 45°, 60°, 90°, 120°, and 150° for all the samples. These measurements for each sample were carried out at the same concentrations as those in the case of the determination of D, but the data for the lowest concentration at θ = 90°, 120°, and 150° for PHIC36 and at θ = 60°, 90°, 120°, and 150° for PHIC77 were not adopted since sufficient photon counts were not obtained at these angles. The sampling times adopted for the determination of D were 5−13 μs for PHIC10, 16−32 μs for PHIC36, and 42−70 μs for PHIC77, and those for the determination of Ω were 0.3−7 μs for PHIC10, 0.5−20 μs for PHIC36, and 0.8−34 μs for PHIC77.

The test solutions of each sample were prepared in the same manner as that in the case of SLS measurements. The values of n_0 at $\lambda_0 = 488$ nm and of η_0 for *n*-hexane at 25.0 °C used to calculate D and Ω are 1.377 and 0.299 cP, respectively. The former value was estimated by a linear interpolation of the plot of n_0 against λ_0^{-2} with the values 1.380 and 1.374 of n_0 at $\lambda_0 = 436$ and 546 nm, respectively.

Viscosity. Viscosity measurements were carried out to determine $[\eta]$ for all the samples in *n*-hexane at 25.0 °C by the use of a four-bulb spiral capillary viscometer of the Ubbelohde type. It is well known that for semiflexible (or stiff) polymers the relative viscosity η_r and hence also $[\eta]$ apparently obtained at a finite rate of shear g are smaller than those at vanishing g. If $[\eta]$ is not very large ($[\eta] \lesssim 50$ dL/g), then η_r (and hence $[\eta]$) at $g = 0$ may be determined by a linear extrapolation of the plot of η_r against g to $g = 0$,[18] where in the present work g may be varied by choosing the bulbs of the viscometer one by one. In all the measurements, the flow time was measured to a precision of 0.1 s, keeping the difference between those of the solvent and solution larger than ca. 20 s. The test solutions were maintained at constant temperature within ±0.005 °C during the measurements. The data for η_r obtained by the above extrapolation to $g = 0$ were treated as usual by the Huggins and Fuoss−Mead plots to determine $[\eta]$.

The test solutions were prepared in the same manner as that in the case of SLS measurements. Density corrections were made in the calculations of c and also of η_r from the flow times of the solution and solvent.

Table 2. Values of $\langle S^2\rangle$, D, $[\eta]$, ρ^{-1}, and Φ for Poly(*n*-hexyl isocyanate) in *n*-Hexane at 25.0 °C

sample	$\langle S^2\rangle$, Å^2	$10^7 D$, cm^2/s	$[\eta]$, dL/g	ρ^{-1}	$10^{-23}\Phi$, mol^{-1}
PHIC10	1.02×10^5	4.80	4.22	0.47_8	0.92_6
PHIC36	5.62×10^5	2.03	15.2	0.48_1	0.88_9
PHIC77	1.35×10^6	1.28	31.1	0.49_2	1.04_3

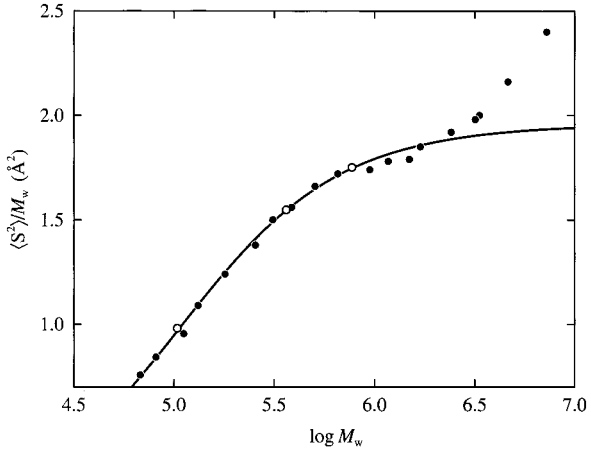

Figure 1. $\langle S^2\rangle/M_w$ against log M_w for PHIC in *n*-hexane at 25.0 °C: (○) present data; (●) data by Murakami et al.[14] The solid curve represents the KP theoretical values calculated from eq 1 with eq 2 with $\lambda^{-1} = 840$ Å and $M_L = 71.5$ Å^{-1}.

Results

Characterization. The values of $\langle S^2\rangle$, D, and $[\eta]$ determined in the present work for the three PHIC samples in *n*-hexane at 25.0 °C are given in the second, third, and fourth columns of Table 2, respectively. We check the utility of these samples by comparing the experimental values given in the table with the corresponding literature values.

We first examine the behavior of $\langle S^2\rangle$. Figure 1 shows plots of $\langle S^2\rangle/M_w$ against the logarithm of M_w for PHIC in *n*-hexane at 25.0 °C. The unfilled circles represent the experimental values obtained in the present work, and the filled circles represent those obtained by Murakami et al.[14] The solid curve represents the KP theoretical values calculated from[19]

$$\langle S^2\rangle = \frac{L}{6\lambda} - \frac{1}{4\lambda^2} + \frac{1}{4\lambda^3 L} - \frac{1}{8\lambda^4 L^2}(1 - e^{-2\lambda L}) \quad (1)$$

for the chain of total contour length L given by

$$L = M/M_L \quad (2)$$

where M is the molecular weight, with $\lambda^{-1} = 840$ Å and $M_L = 71.5$ Å^{-1}.[14] As seen from the figure, the present data agree well with those by Murakami et al.[14] within experimental error, and the data of the two groups well

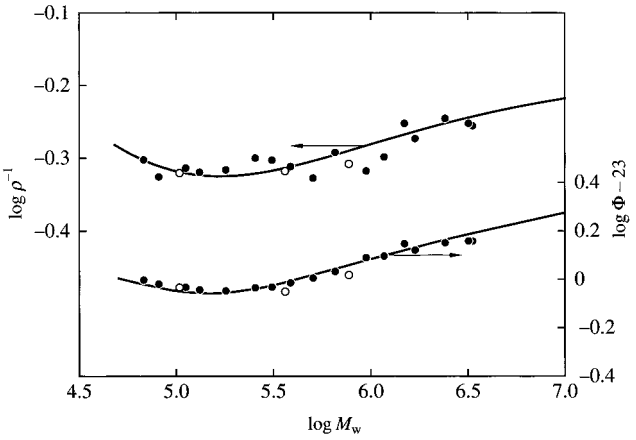

Figure 2. Double-logarithmic plots of ρ^{-1} and Φ against M_w for PHIC in *n*-hexane at 25.0 °C: (○) present data; (●) data by Murakami et al.[14] The solid curves represent the respective KP theoretical values (see the text).

follow the theoretical curve in the range of $M_w \lesssim 3 \times 10^6$. Note that the excluded-volume effect becomes appreciably large for $M_w \gtrsim 3 \times 10^6$.

Next we examine the behavior of the reduced hydrodynamic radius ρ^{-1} and volume Φ instead of the transport coefficients D and $[\eta]$ themselves, respectively. These two reduced quantities are defined by[2]

$$\rho^{-1} = R_H/\langle S^2\rangle^{1/2} \tag{3}$$

$$\Phi = V_H/\langle S^2\rangle^{3/2} \tag{4}$$

where R_H and V_H are the hydrodynamic radius and (molar) volume, respectively, defined by

$$R_H = k_B T/6\pi\eta_0 D \tag{5}$$

$$V_H = 6^{-3/2} M[\eta] \tag{6}$$

The values of ρ^{-1} and Φ calculated from eqs 3−6 with the values of $\langle S^2\rangle$, D, and $[\eta]$ given in Table 2 are also given in its fifth and sixth columns, respectively.

Figure 2 shows double-logarithmic plots of ρ^{-1} and Φ against M_w for PHIC in *n*-hexane at 25.0 °C. The unfilled circles represent the values given in Table 2, and the filled circles represent those calculated with the values of $\langle S^2\rangle$, s, and $[\eta]$ obtained by Murakami et al.,[14] where we note that

$$R_H = (1 - \bar{v}\rho_0)M/6\pi\eta_0 N_A s \tag{7}$$

with $\bar{v}$ the partial specific volume of the polymer, ρ_0 the density of the solvent, and N_A the Avogadro constant. The solid curves represent the KP theoretical values calculated from eqs 3 and 4 with the values of $\langle S^2\rangle$ calculated from eq 1 with eq 2 and with those of R_H and V_H calculated from eqs 5 and 6, respectively, where the necessary theoretical values of D and $[\eta]$ have been calculated from eqs 6.127 and 6.123 of ref 2, respectively, for the KP cylinder model with the cylinder diameter d. The values of λ^{-1} and M_L used for the calculations are the same as above, and that of d is 25 Å for D and 16 Å for $[\eta]$. (Recall that the difference between the d values arises from the preaveraging approximation to the Oseen tensor.[2]) As in the case of $\langle S^2\rangle$, the present data agree well with those by Murakami et al.[14] within experimental error for both ρ^{-1} and Φ, and the data of the two groups well follow the respective theoretical curves. We note that the data obtained by Murakami et al.[14] for the two samples with the highest M_w in Figure 1 have been omitted here, since the excluded-volume effect is appreciably large there, as mentioned above. The characterization above for the present PHIC samples allows us to proceed to study Ω.

Table 3. Values of $\Omega(k)$ and $\eta_0\Omega(k)/k_BTk^3$ for Poly(*n*-hexyl isocyanate) in *n*-Hexane at 25.0 °C

sample	θ, deg	10^3k, Å^{-1}	$\Omega(k)$, s^{-1}	$\eta_0\Omega(k)/k_BTk^3$
PHIC10	20	0.616	$1.8_5 \times 10^3$	0.575
	25	0.767	$2.8_6 \times 10^3$	0.460
	30	0.917	$4.1_8 \times 10^3$	0.392
	45	1.357	$9.1_4 \times 10^3$	0.266
	60	1.772	$1.5_9 \times 10^4$	0.206
	90	2.507	$3.6_1 \times 10^4$	0.166
	120	3.070	$5.5_4 \times 10^4$	0.139
	150	3.424	$6.9_2 \times 10^4$	0.125
PHIC36	20	0.616	$8.2_3 \times 10^2$	0.256
	25	0.767	$1.3_0 \times 10^3$	0.209
	30	0.917	$1.8_1 \times 10^3$	0.170
	45	1.357	$4.2_6 \times 10^3$	0.124
	60	1.772	$8.3_8 \times 10^3$	0.109
	90	2.507	$2.1_1 \times 10^4$	0.097_3
	120	3.070	$3.5_1 \times 10^4$	0.088_0
	150	3.424	$4.7_6 \times 10^4$	0.086_0
PHIC77	20	0.616	$5.0_3 \times 10^2$	0.157
	25	0.767	$8.1_8 \times 10^2$	0.131
	30	0.917	$1.2_5 \times 10^3$	0.117
	45	1.357	$3.2_4 \times 10^3$	0.094_1
	60	1.772	$6.8_4 \times 10^3$	0.089_1
	90	2.507	$1.8_7 \times 10^4$	0.086_3
	120	3.070	$3.3_6 \times 10^4$	0.084_1
	150	3.424	$4.4_0 \times 10^4$	0.079_6

First Cumulant. The first cumulant $\Omega(k)$ (as a function of the magnitude k of the scattering vector) defined as the initial decay rate of the dynamic structure factor $S(k,t)$ (as a function of k and time t), i.e., $\Omega(k) \equiv -[\mathrm{d} \ln S(k,t)/\mathrm{d}t]_{t=0}$, may be written in terms of the normalized autocorrelation function $g^{(2)}(t)$ of the scattered light intensity observed in DLS measurements as follows:

$$\Omega(k) = -\left[\frac{\mathrm{d}}{\mathrm{d}t}\left\{\frac{1}{2}\ln[g^{(2)}(t) - 1]\right\}\right]_{t=0} \tag{8}$$

We note that k is related to the scattering angle θ by

$$k = (4\pi/\tilde{\lambda})\sin(\theta/2) \tag{9}$$

with $\tilde{\lambda}$ the wavelength of the incident light in the solvent.

As in the case of the previous study of Ω for flexible polymers,[4] the initial tangent of (1/2) $\ln[g^{(2)}(t) - 1]$ at each θ for each test solution has been determined by extrapolating the data to $t = 0$ by the use of the Fortran program package CONTIN[17] supplied by Brookhaven Instruments. Then the values of the initial slope so determined at finite concentrations at each θ for each sample have been linearly extrapolated to $c = 0$ to determine Ω at infinite dilution. In Table 3 are given the values of $\Omega(k)$ and $\eta_0\Omega(k)/k_BTk^3$ so determined.

Figure 3 shows plots of $\eta_0\Omega(k)/k_BTk^3$ against $\bar{k} \equiv \langle S^2\rangle^{1/2}k$. The unfilled circles, triangles, and squares represent the present experimental values for the samples PHIC10, PHIC36, and PHIC77, respectively, in *n*-hexane at 25.0 °C. The filled circles and squares represent the previous experimental values for a-PS in cyclohexane at 34.5 °C (Θ)[4] and the literature values reported by Soda and Wada[20] for linear ColEl DNA with

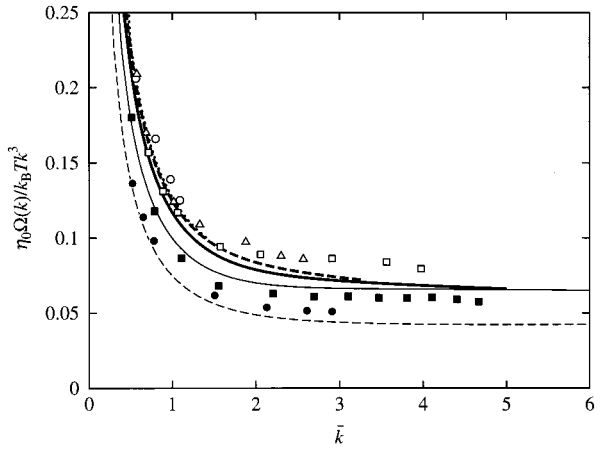

Figure 3. $\eta_0\Omega(k)/k_BTk^3$ against the reduced magnitude $\bar{k}$ of the scattering vector. The unfilled circles, triangles, and squares represent the present experimental values for the PHIC samples PHIC10, PHIC36, and PHIC77, respectively, in *n*-hexane at 25.0 °C. Also are shown the results for a-PS in cyclohexane at 34.5 °C (Θ)[4] (filled circles) and those obtained by Soda and Wada[20] for ColEl DNA in 0.15 M NaCl at 25.0 °C (filled squares). The heavy dotted, dashed, and solid curves represent the KP theoretical values for the PHIC samples PHIC10, PHIC36, and PHIC77, respectively, and the light solid one represents those for DNA. The light dashed curve represents the HW theoretical values for a-PS (see the text).

L = ca. 2.24 μm in 0.15 M NaCl (with 0.015 M trisodium citrate) at 25.0 °C. It is seen that the present data points for PHIC nearly form a single-composite curve but are higher than those for a-PS and DNA. In the figure the curves represent the KP and HW theoretical values, which are discussed in the next section.

Discussion

HW Theory. We begin by giving a short sketch of the (discrete) dynamic HW chain model (and also of the KP chain as its special case).[2] The model is composed of N identical rigid subbodies joined successively with bonds of fixed length a, where their centers are located nearly on the contour of the continuous HW chain of length L and each subbody has translational and rotatory friction coefficients ζ_t and ζ_r. Specifically, the pair potential between two successive subbodies is chosen so that the static behavior of the dynamic model becomes identical with that of the continuous HW chain.[2] The latter is an elastic wire model with both bending and torsional energies. In particular, for flexible chains, the bending and torsional force constants associated with the two kinds of elastic energies may be set equal to each other. The HW chain may then be described in terms of the static stiffness parameter λ^{-1} (equal to the bending force constant multiplied by $2/k_BT$) and the constant differential-geometrical curvature κ_0 and torsion τ_0 of the characteristic helix, i.e., the regular helical form taken by the contour of the chain at the minimum zero of its total elastic energy (along with M_L). A special case of the HW chain with $\kappa_0 = 0$ but with the two (different) force constants is the *generalized* KP chain, which is the model for most stiff (or semiflexible) chains (with large λ^{-1}). If the torsion of the chain is not considered, the generalized KP chain is identical with the *original* KP chain (with $\kappa_0 = 0$ and with vanishing torsional force constant) and the parameter τ_0 does not appear. In what follows, therefore, both the original and generalized KP chains are referred to simply as the KP chain. The number of subbodies N in the discrete model may be related to L by $L = N\Delta s$, where Δs is the contour length per subbody and is uniquely related to a.

Now, for the dynamic HW chain (without excluded volume) such that each subbody has an isotropic scatterer, the dimensionless quantity $\eta_0\Omega(k)/k_BTk^3$ may be written in the form[1,2]

$$\eta_0\Omega(k)/k_BTk^3 = (1/6\pi)[\rho/\bar{k} + F(\bar{k})/\bar{k}] \qquad (10)$$

where $F(\bar{k})$, which is given by eq 10.66 of ref 2, may be expressed in terms of the solutions of the eigenvalue problem associated with the diffusion operator appearing in the coarse-grained version of the diffusion equation (in the diffusion equation for the c-HW chain),[2,3] along with the static structure factor, $\langle S^2\rangle$, and the mean-square end-to-end distance of the chain. The dimensionless quantity $F(\bar{k})$ as a function of $\bar{k}$ (for flexible chains) depends on the dimensionless parameters $\lambda^{-1}\kappa_0$, $\lambda^{-1}\tau_0$, $\lambda\Delta s$ (or λa), N, $r_1 = \zeta_t/3\pi\eta_0 a$, and $r_2 = \zeta_r/a^2\zeta_t$ and may be evaluated numerically. For the present KP (stiff) chain, whose torsion dynamics is not considered, $\lambda^{-1}\kappa_0$ is set equal to zero and $\lambda^{-1}\tau_0$ does not appear.

We then examine the behavior of the theoretical Ω for the KP chains corresponding to the three PHIC samples, whose additional model parameters are determined in the following. As previously mentioned,[1] the KP touched-bead model is suitable for a study of the dynamics of typical stiff (or semiflexible) chains. The diameter d_b (=a) of the spherical bead (subbody) may be estimated to be 29 Å from the relation $d = 0.861d_b$ for the conversion between the cylinder and touched-bead models[2,21] with the value 25 Å of the cylinder diameter d determined from s (D).[14] This a value and the λ^{-1} value given in the last section give $\lambda\Delta s$ ($\simeq\lambda a$) = 0.035. We note that the above conversion factor 0.861 evaluated from the rotatory diffusion coefficient[21] has been adopted as before[1] instead of the factor 0.891 evaluated from D,[21] since the long-wavelength internal motions rather than the entire translational motion make a contribution to $F(\bar{k})$. The contour lengths L for the samples PHIC10, PHIC36, and PHIC77 are calculated to be 1450, 5080, and 10780 Å, respectively, from their M_w values given in Table 1 along with the M_L value given in the last section. The numbers of beads N_b (= $N = L/\Delta s \simeq L/a$) in the chains corresponding to PHIC10, PHIC36, and PHIC77 are then 50, 175, and 371, respectively. As for r_1 and r_2, we use the values 1 and 1/3, respectively, assuming as before[1] that ζ_t and ζ_r for the spherical bead take the Stokes values. For the theoretical values of ρ on the right-hand side of eq 10, we use those for the cylinder model shown in Figure 2, i.e., 2.085, 2.059, and 1.945 for PHIC10, PHIC36, and PHIC77, respectively.

Figure 4 shows plots of $\eta_0\Omega(k)/k_BTk^3$ against $\bar{k}$. The dotted, dashed, and solid curves represent the theoretical values for the KP touched-bead chains corresponding to the samples PHIC10, PHIC36, and PHIC77, respectively. In contrast to the previous result shown in Figure 3 of ref 1 that $\eta_0\Omega(k)/k_BTk^3$ is independent of chain length for $\bar{k} \lesssim 6$ for flexible chains with very large M, the difference between the present plots for the three KP chains is not negligibly small in the same range of $\bar{k}$. The difference in the range of $\bar{k} \lesssim 1$ is due to that in ρ between the above three chains, while the behavior of the plot in the range of larger $\bar{k}$ is mainly determined by $F(\bar{k})$. Figure 4 is also to be compared with Figure 4

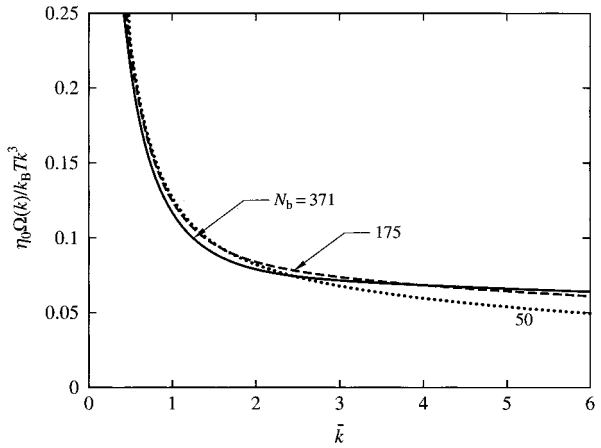

Figure 4. KP theoretical values of $\eta_0\Omega(k)/k_BTk^3$ plotted against the reduced magnitude $\tilde{k}$ of the scattering vector for PHIC for the indicated values of N_b (see the text).

of ref 1. The plots displayed in the latter for stiff chains are those for three KP touched-bead chains with the same N_b (=999) but with different λ^{-1}; the plot moves upward as λ^{-1} is increased (or the reduced contour length λL is decreased).

Comparison with Theory. In Figure 3, the theoretical values for the above three KP touched-bead chains are also plotted in the ranges of $\tilde{k}$ where the corresponding data exist, the heavy dotted, dashed, and solid curves representing the values for the samples PHIC10, PHIC36, and PHIC77, respectively. Here, we have also reproduced the plot of theoretical values (light solid curve) for the KP touched-bead chain corresponding to DNA from ref 1 and that (light dashed curve) for the HW chain corresponding to a-PS from ref 4. The theoretical values for DNA were calculated with $\lambda\Delta s = 0.026$, $N_b = 772$, and $\rho = 1.64$ in the same manner as that in the case of PHIC above. For the calculation for a-PS, for which the subbody corresponds to the repeat unit and may be represented by an oblate spheroid rather than a spherical bead, the values 1 and 10 were used for r_1 and r_2, respectively. The other parameter values used for a-PS are $\lambda^{-1}\kappa_0 = 3.0$, $\lambda^{-1}\tau_0 = 6.0$, $\lambda\Delta s = 0.14$, and $N \simeq 10^4$. For flexible chains, theory fails to give a correct value of ρ, as mentioned in the Introduction, so that its experimental value 1.30_5 was used for a-PS.

It is seen from Figure 3 that the behavior of $\eta_0\Omega(k)/k_BTk^3$ for the three kinds of polymers may be rather satisfactorily explained by the theory. Precisely, for PHIC, the observed $\eta_0\Omega(k)/k_BTk^3$ decreases with increasing M_w in the range where the data exist, as predicted by the theory, although we have already mentioned that the data points nearly form a single-composite curve. Both the experimental and theoretical values for DNA are smaller than the corresponding values for PHIC despite the fact that DNA ($\lambda^{-1} = 1100$ Å) is stiffer than PHIC ($\lambda^{-1} = 840$ Å). This arises from the fact that ρ is smaller for DNA ($\rho = 1.64$) than for PHIC ($\rho \simeq 2$). This difference in ρ is mainly due to that in chain length. We note that even for very large M, the plateau height of $\eta_0\Omega(k)/k_BTk^3$ and also ρ still depend somewhat on chain stiffness and local chain conformation.[2,4,15]

As in the case of a-PS, the theoretical values are somewhat smaller than the experimental ones for PHIC in the range of large $\tilde{k}$. This (minor) defect may be regarded as arising from the effect of the preaveraging approximation to the Oseen tensor on the internal motions, as mentioned in the Introduction. In contrast to the cases of PHIC and a-PS, the theoretical values are larger than the experimental ones for DNA. As mentioned in the previous paper,[1] the experimental values for DNA may be considered to be somewhat too small.

Conclusion

The first cumulant $\Omega(k)$ as a function of the magnitude k of the scattering vector has been determined for PHIC as a typical semiflexible polymer in *n*-hexane at 25.0 °C to investigate the effect of chain stiffness on Ω. It is shown that the present data for PHIC along with the previous data for a-PS and the literature data for DNA are consistent with the HW theoretical prediction for the dimensionless quantity $\eta_0\Omega(k)/k_BTk^3$ as a function of the reduced magnitude $\langle S^2\rangle^{1/2}k$ of the scattering vector. In general, this dimensionless quantity appreciably depends on the kind of polymer even for flexible polymers. Thus, the (dynamic) HW chain model has proved to be of use also for a study of Ω for both flexible and semiflexible polymers.

References and Notes

(1) Yoshizaki, T.; Osa, M.; Yamakawa, H. *J. Chem. Phys.* **1997**, *106*, 2828.
(2) Yamakawa, H. *Helical Wormlike Chains in Polymer Solutions*; Springer: Berlin, 1997.
(3) Yoshizaki, T.; Yamakawa, H. *J. Chem. Phys.* **1996**, *104*, 1120.
(4) Sawatari, N.; Yoshizaki, T.; Yamakawa, H. *Macromolecules* **1998**, *31*, 4218.
(5) Kratky, O.; Porod, G. *Recl. Trav. Chim. Pays-Bas* **1949**, *68*, 1106.
(6) Norisuye, T. *Prog. Polym. Sci.* **1993**, *18*, 543 and references cited therein.
(7) Zimm, B. H. *Macromolecules* **1980**, *13*, 592.
(8) Yamakawa, H.; Yoshizaki, T. *J. Chem. Phys.* **1989**, *91*, 7900.
(9) Burchard, W.; Schmidt, M.; Stockmayer, W. H. *Macromolecules* **1980**, *13*, 580.
(10) Benmouna, M.; Akcasu, A. Z. *Macromolecules* **1980**, *13*, 409.
(11) Aharoni, S. M. *Macromolecules* **1979**, *13*, 409.
(12) Deželić, Gj.; Vavra, J. *Croat. Chem. Acta* **1966**, *38*, 35.
(13) Berry, G. C. *J. Chem. Phys.* **1966**, *44*, 4550.
(14) Murakami, H.; Norisuye, T.; Fujita, H. *Macromolecules* **1980**, *13*, 345.
(15) Konishi, T.; Yoshizaki, T.; Yamakawa, H. *Macromolecules* **1991**, *24*, 5614.
(16) Osa, M.; Abe, F.; Yoshizaki, T.; Einaga, Y.; Yamakawa, H. *Macromolecules* **1996**, *29*, 2302.
(17) Provencher, S. W. *Comput. Phys. Commun.* **1982**, *27*, 213.
(18) Kashiwagi, Y.; Norisuye, T.; Fujita, H. *Macromolecules* **1981**, *14*, 1220.
(19) Benoit, H.; Doty, P. *J. Phys. Chem.* **1953**, *57*, 1953.
(20) Soda, K.; Wada, A. *Biophys. Chem.* **1984**, *20*, 185.
(21) Yamakawa, H. *Macromolecules* **1983**, *16*, 1928.

MA992075X